ME 429
Mechanical & Thermal Design

Weight Compensation Mechanism
for an Elastic Metamaterial
Project Report

Ege ORAY
Yankı KIRAN
Yiğit Günsür ELMACIOĞLU

23.01.2022

1 Abstract

This report discusses weight compensation in elastic metamaterials with phononic band gaps introduced by inertial amplification. First, it is demonstrated through relevant practical work that the inertial amplification mechanism locks up under axial loads, including its own weight, making it unable to function. Two approaches are then suggested to provide the necessary forces to compensate for such axial loads: pre-bending the long flexures before installing them in place to create opposing initial stresses, and rotating one of the fixed ends of each long flexure to create reaction forces and moments at the fixed ends. For the former, the magnitudes of the necessary forces to compensate for the axial loads are related to the amount of initial plastic deformation that is needed to be introduced in the flexures through static structural analysis. For the latter, the necessary forces are related to the amount of rotation that is needed to be imposed at one of the fixed ends. In the end, the two approaches are combined into one, where pre-bent flexures are installed to provide the majority of the necessary forces and rotating one of their fixed ends allows for fine-tuning. An examplary design which can carry an additional 10 N of axial load as well as its own weight is given. Modal analyses show that such an approach does not affect the band gaps by much, and the wide band gaps at low frequencies are still present.

Table of Contents

1 Abstract

List of Tables

List of Figures

2 Introduction **1**

2.1 Metamaterials and Phononic Band Gaps 1

2.2 Problem Definition 4

3 Overview of Possible Solutions **5**

4 Design and Analysis **7**

4.1 Final Design 7

4.2 Finite Element Analysis 9

4.2.1 Mesh Specs 9

4.2.2 Analysis and Results 12

4.3 Analytical Formulation 17

4.4 Maximum Allowable External Load 19

4.5 Cost Analysis 19

5 Conclusion **20**

6 References **21**

A Technical Drawings **22**

List of Tables

1 Optimized dimensions of the mechanism for maximum Band Gap 3
2 Required horizontal reaction force for negligible deformation 14
3 Comparison of reaction forces for analytical and finite element methods . . 18

List of Figures

2.1 (a) Negative-refractive-index [1] and (b) Negative-Poisson's-ratio [2] . . . 1
2.2 The inertial amplification mechanism [4] 2
2.3 The inertial amplification mechanism [3] 2
2.4 Exaggerated drawing of the inertial amplification mechanism [3] 3
2.5 Experimental Setup [3] 3
2.6 The first and second natural frequencies of the system [3] 4
2.7 The system when it is compressed 4
3.1 Simplified Free Body Diagram 5
3.2 First Design Alternative 5
3.3 Initially deflected long flexure 6
3.4 Adjustable boundary condition with rotating fixed support 6
4.1 Final design when the long flexure is straight 7
4.2 Final design 17 degree rotation 7
4.3 Final design fixed with a nut 7
4.4 Initially bent beam before mounting 8
4.5 Opening slit into the shoulder bolt 8
4.6 Shoulder bolt with the slit at the middle 8
4.7 (a) Structured and (b) unstructured mesh examples for a cube [5] 9
4.8 18 Bodies forming a single part 10
4.9 Close-up of small flexure mesh 10
4.10 Long flexure when undeformed 11
4.11 Long flexure when deformed 11
4.12 General Mesh Settings 11
4.13 General Mesh View 1 12
4.14 General Mesh View 2 12
4.15 Natural frequencies and mode shapes 12

4.16 Compression under its own weight 13
4.17 10N External Force added 13
4.18 The forces and moments applied by the flexure 14
4.19 18.2mm deflected beam 15
4.20 Successful weight compensation 15
4.21 Natural frequencies and mode shapes for 5 degrees of rotation 16
4.22 Natural frequencies and mode shapes for 17 degrees of rotation 16
4.23 Natural frequencies and mode shapes for 28 degrees of rotation 16
4.24 Original FRF 16
4.25 5 degree FRF 16
4.26 17 degree FRF 17
4.27 28 degree FRF 17
4.28 Free-Body of deflection of the long flexure 17

2 Introduction

2.1 Metamaterials and Phononic Band Gaps

It would be convenient to start the report with a quick description of metamaterials. They are artificial materials produced to have properties that go beyond properties of natural materials. They usually have periodic structures designed in such a way that they interact with their environment in unique ways. In Figure 2.1 two examples are given – the first one is a metamaterial with a negative refractive index, and the other one is a metamaterial with a negative Poisson's ratio.

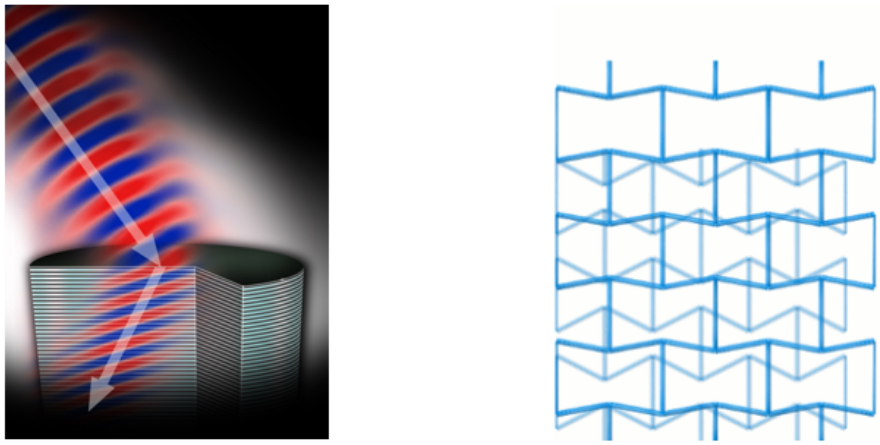

Figure 2.1: (a) Negative-refractive-index [1] and (b) Negative-Poisson's-ratio [2]

The type of metamaterial this report focuses on is elastic metamaterials with phononic band gaps, with the term phononic referring to vibrational motion in general such as acoustic waves, elastic waves etc. What these materials do is that they attenuate the transmission of vibration in a certain frequency range. This frequency range is called the band gap and its width is function of the lower and upper limits of the gap. The width of the band gap increases as these limits get further apart. Elastic metamaterials with phononic band gaps can be made use of in acoustic waveguides, mechanical filters and isolators [3].

When we examine how this behavior is achieved, we see that there are examples making use of the Bragg scattering and local resonance phenomena but both of these methods are limited on their practicality as they both require the use of heavy materials to achieve band gaps at low frequencies [4].

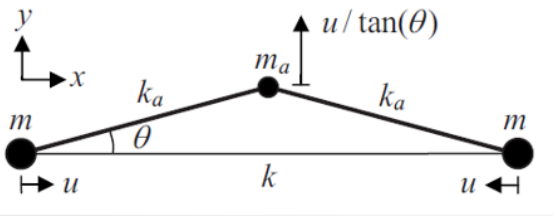

Figure 2.2: The inertial amplification mechanism [4]

A more recent approach to achieving phononic band gaps (Yilmaz et al. 2007) involves the idea of inertial amplification where band gaps at low frequencies are achieved not by adding extra mass but by distributing the present mass and linking them together in a hinge mechanism. Figure 2.2 illustrates the operating principle through a simple system consisting of three point masses linked together by two rigid beams and a spring. When the end points displace horizontally by an amount u, the middle point has to displace vertically by an amount $u/\tan(\theta)$ due to geometry. As θ gets smaller, this vertical displacement gets very large. But a large displacement requires a large amount of energy which may not be present in the system. So in a way m_a limits the motion of the system by acting heavier than it is.

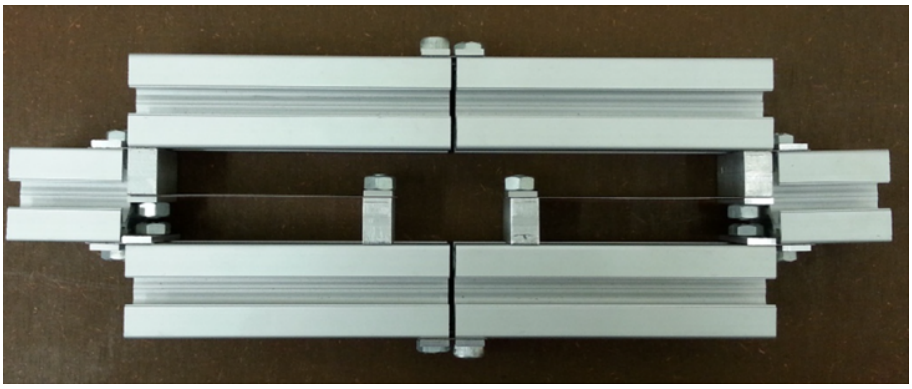

Figure 2.3: The inertial amplification mechanism [3]

To achieve inertial amplification, Yilmaz created a mechanism shown in Figure 2.3 which holds the record of the widest band gap region. This mechanism consists of aluminum sigma profiles and thin steel flexure hinges. In Figure 2.3, the flexure hinges cannot be seen easily. An exaggerated drawing can be seen in Figure 2.4. The thin flexures are numbered as 2,4 and 5.

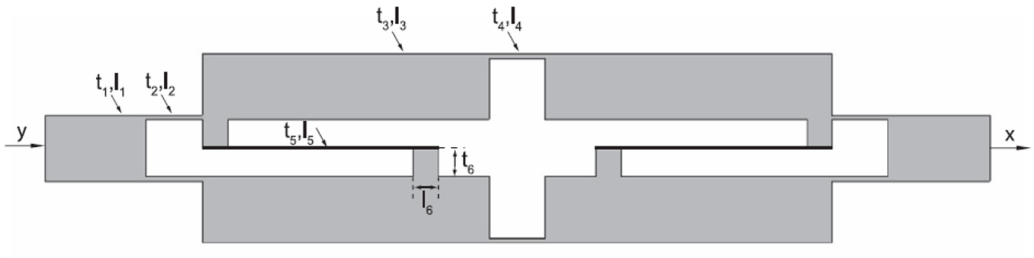

Figure 2.4: Exaggerated drawing of the inertial amplification mechanism [3]

Table 1: Optimized dimensions of the mechanism for maximum Band Gap

$\mathbf{L}_1$	36 mm	$\mathbf{t}_1$	30 mm
$\mathbf{L}_2$	2 mm	$\mathbf{t}_2$	0.2 mm
$\mathbf{L}_3$	102 mm	$\mathbf{t}_3$	30 mm
$\mathbf{L}_4$	2 mm	$\mathbf{t}_4$	0.2 mm
$\mathbf{L}_5$	66 mm	$\mathbf{t}_5$	0.25 mm
$\mathbf{L}_6$	9 mm	$\mathbf{t}_6$	14.925 mm

The amplitude reduction effect of this mechanism is proven by experiment. The experimental setup can be seen in Figure 2.5. An input force is given from one end and measured by the force transducer inside the hammer. The resultant output acceleration is measured with an accelerometer.

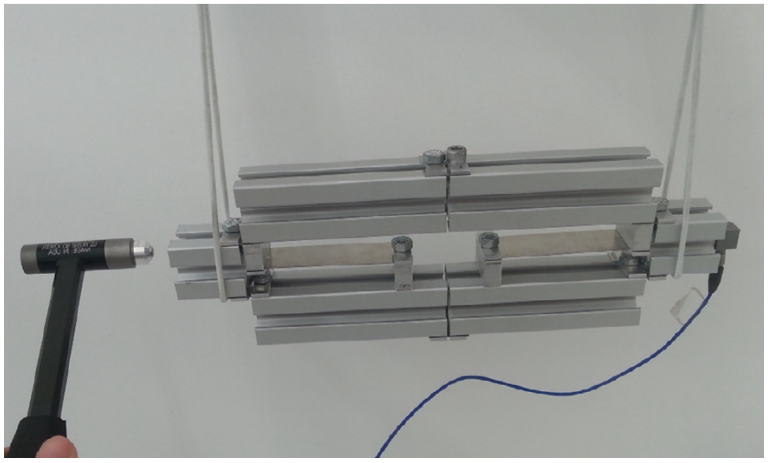

Figure 2.5: Experimental Setup [3]

The first and second natural frequencies and mode shapes achieved by Yilmaz's mechanism are given in Figure 2.6. They characterize the first band gap of the system.

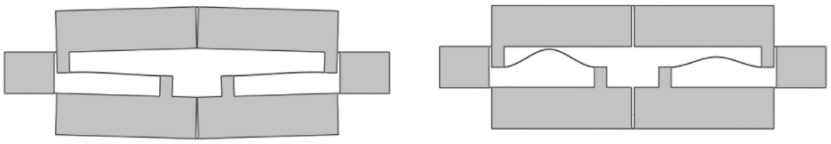

(a) 6.9 Hz (b) 303.6 Hz

Figure 2.6: The first and second natural frequencies of the system [3]

2.2 Problem Definition

Although the system works well in the horizontal plane - when the setup is similar to Figure 2.5 - the system can not support any load in the vertical direction including its own weight which renders it unable to function properly. When compressed, the edges of the sigma profiles come in contact and the mechanism does not work as intended. The situation can be seen clearly in Figure 2.7 where the red arrows show the sigma profiles coming in contact.

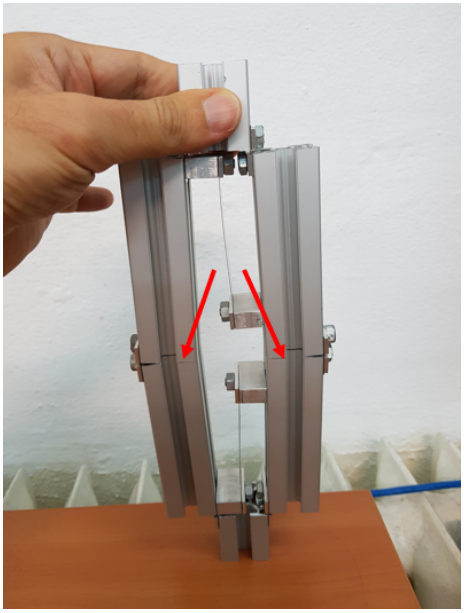

Figure 2.7: The system when it is compressed

This problem limits the use of this mechanism only to horizontal plane. To be able to construct 3D arrays as future implementations, a weight compensation mechanism is essential for this system. Furthermore, this weight compensation mechanism must not alter the band gap significantly.

3 Overview of Possible Solutions

The easiest way to achieve weight compensation is to create initial stresses in the long flexures which will cause reaction forces either in horizontal or vertical direction. You can see in Figure 3.1 that the reaction forces have the effect to pull point B to the left and point A to the right.

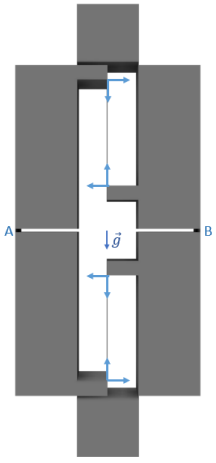

Figure 3.1: Simplified Free Body Diagram

To create these forces, we came up with different conceptual designs. In the first one, we have a flexure which is longer than it should be and by rotating the yellow pin, we can change the length and create a tensile stress in the flexure which results in vertical reaction force. But after ANSYS Static Structural analysis, the effect of the vertical force turned out to be negligible. Therefore, horizontal forces can compensate the gravity more effectively.

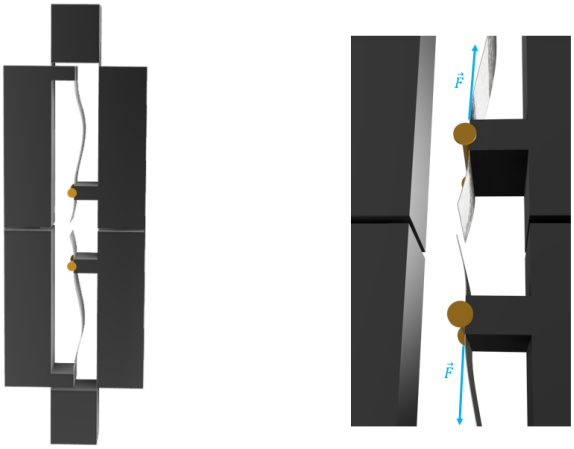

Figure 3.2: First Design Alternative

The second design aims to create horizontal force. We planned to deflect the flexure beforehand and fix it to the supports. As a result, we will have bent beams which create horizontal reaction forces. However, this design is not easily adjustable for different loading configurations since deflecting beam by a specific amount is not easy to measure.

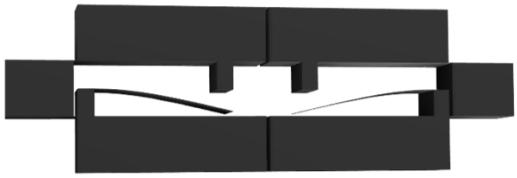

Figure 3.3: Initially deflected long flexure

Having different boundary conditions at one end with a gear type changeable fixed support, we can change angle theta and hence the reaction forces. For example, if we increase angle theta, we should have higher force. The reason for gear teeth is to prohibit flexure from turning after it is placed.

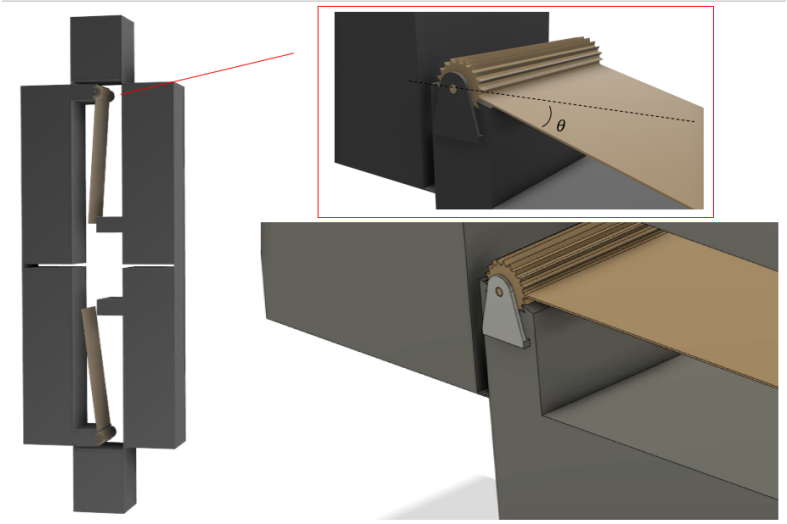

Figure 3.4: Adjustable boundary condition with rotating fixed support

Even though the gear type mechanism offers an adjustable force, it is not possible to change the angle while there is a load on the mechanism. So, in our final design, we tried to merge initial bending and angle adjustment concepts into one with better implementation.

4 Design and Analysis

4.1 Final Design

In the previous section, we claimed to have a design making use of both initial deflection and support angle adjustment. To overcome the problem of adjustment without completely removing the long flexure, a shoulder bolt will be used in the final design.

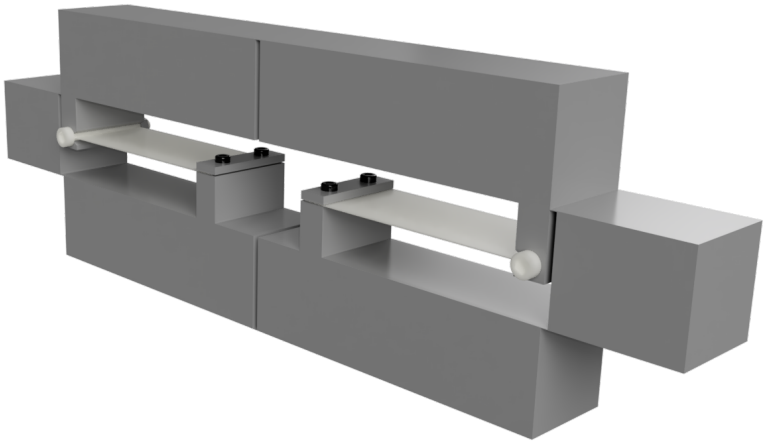

Figure 4.1: Final design when the long flexure is straight

The allen screw head will help to adjust the rotation angle precisely from -30° to +30°. When enough force is generated, the angle will be fixed by turning the nut at the threaded end of the shoulder bolt.

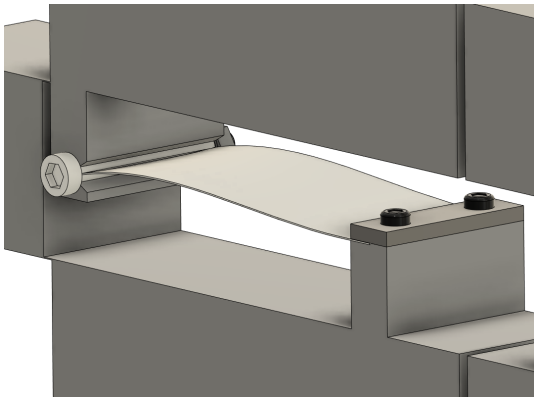

Figure 4.2: Final design 17 degree rotation

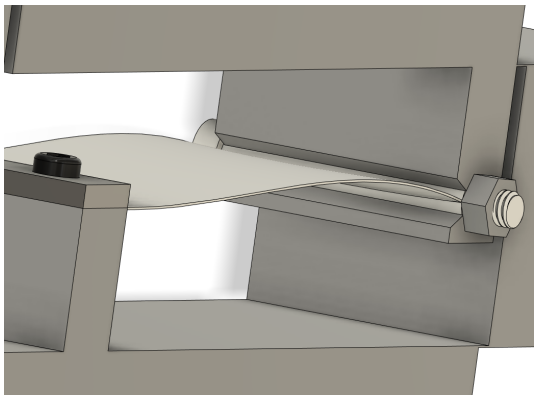

Figure 4.3: Final design fixed with a nut

As it will be explained in Section 4.2.2, rotation does not affect the band gap significantly up to 17 degrees. Although it is enough for weight compensation, using an initially bent

beam can increase the maximum allowable load on the mechanism without any expense on the band gap, since after mounting without any rotation angle, Figure 4.4 exactly becomes Figure 4.1.

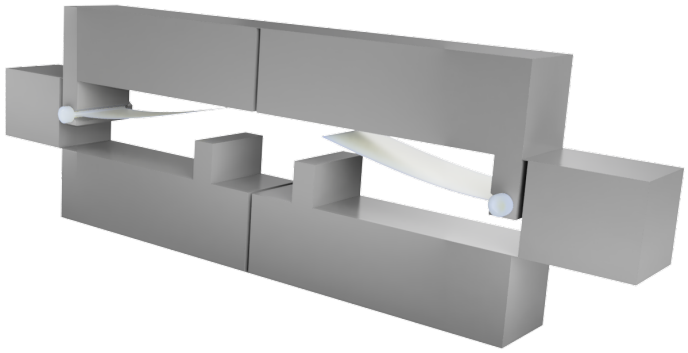

Figure 4.4: Initially bent beam before mounting

It is worth noting that by bent beam, we mean plastic deformation caused by large deflection. To achieve such a shape, we first have to bend the beam up to plastic range, then release it. It will not go back to its initial shape which is straight, but will stay as in Figure 4.4 , permanently deformed.

Black bolts in Figures 4.1-4.2-4.3 also have allen screw heads to facilitate assembly since there is not much space above them. The long flexures will be squeezed into the slits in the shoulder bolts opened by milling cutter. This manufacturing method is proved during initial testing as shown in Figure 4.5.

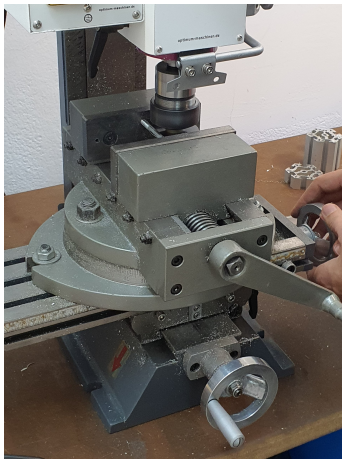

Figure 4.5: Opening slit into the shoulder bolt

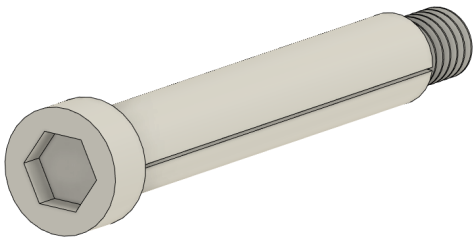

Figure 4.6: Shoulder bolt with the slit at the middle

4.2 Finite Element Analysis

4.2.1 Mesh Specs

The reliability and accuracy of the finite element method strongly correlate with the quality of the mesh structure. Therefore, in this section, details of the mesh will be elaborated in terms of method and element size.

There are mainly two types of mesh categories, namely structured and unstructured. In the former, the connectivity or neighborhood relations are more apparent and thus, less data has to be stored for each cell. On the other hand, in the unstructured mesh, there is no uniform order in the arrangement of the cells. Examples of these categories can be seen in Figure 4.7.

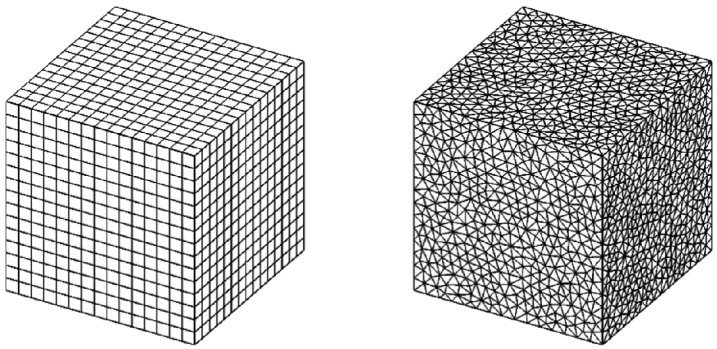

Figure 4.7: (a) Structured and (b) unstructured mesh examples for a cube [5]

When available, structured meshes increase performance and reduce overall number of elements without losing accuracy and reliability. The geometry proposed in this study is a combination of rectangular prisms and it is highly appropriate to use structured mesh. Since the connection parts, like long and short flexures, have 0.2mm thickness, an unstructured mesh with enough number of elements in those regions has over half a million total number of elements. Thus, analyses using unstructured mesh would take hours.

ANSYS Mechanical fails to construct a structured mesh without slight alteration in the geometry. To specify rectangular prisms more obviously, first the part must be sliced into smaller bodies and then formed into a single part to specify that these still belong to the same part. The part after several slicing operations can be seen in Figure 4.8.

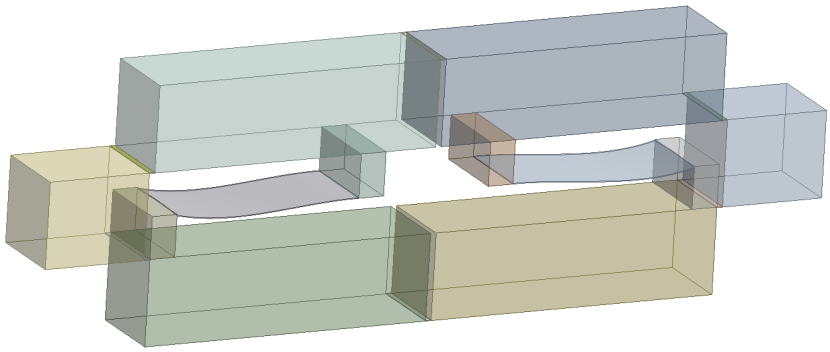

Figure 4.8: 18 Bodies forming a single part

From now on ANSYS Mechanical can construct a structured mesh without effort. However, regions with low thickness have to be adjusted further for accurate results since those strongly affect the modal analysis because they are the only non-rigid part of this part. Addition of edge sizing with 3 divisions vertically and 5 divisions horizontally for small flexures give us the mesh shown in Figure 4.9.

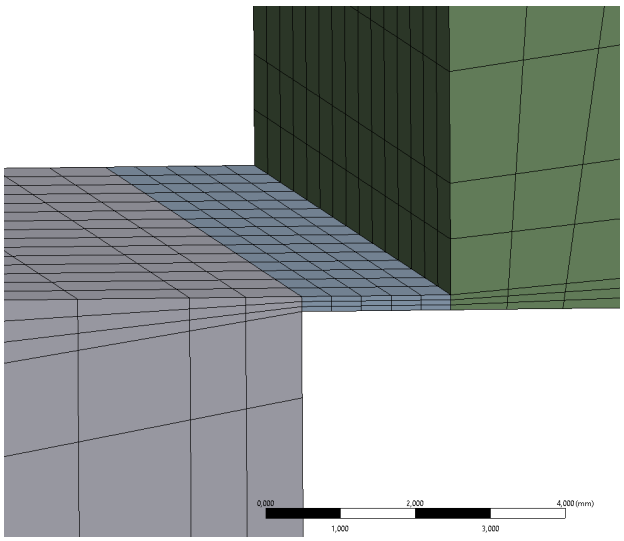

Figure 4.9: Close-up of small flexure mesh

For the long flexures, there are two cases, undeformed and deformed. When the long flexures are straight, it is easier to construct the mesh. 3 divisions vertically are used for the undeformed case. On the contrary, 2 divisions vertically is used for the deformed case.

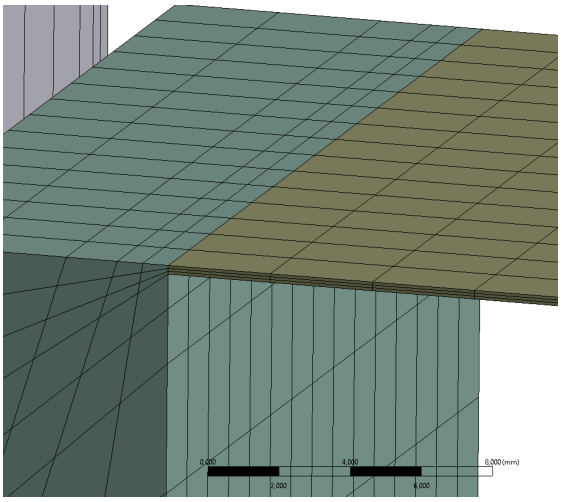

Figure 4.10: Long flexure when undeformed

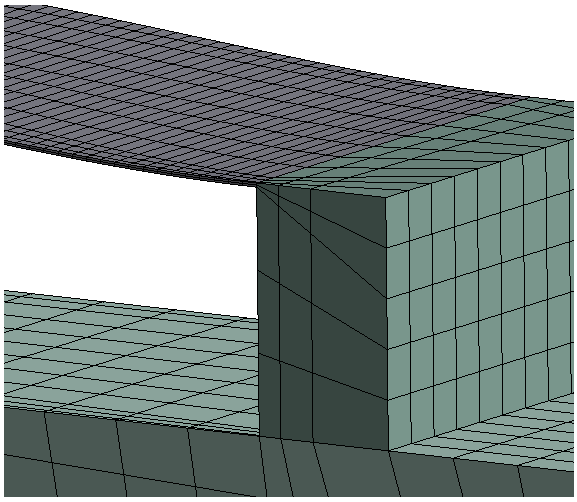

Figure 4.11: Long flexure when deformed

In general sizing settings, the element size is set to 3mm with slow transition. Settings can be seen in Figure 4.12.

Details of "Mesh"

Display	
Display Style	Use Geometry Setting
Defaults	
Physics Preference	Mechanical
Element Order	Program Controlled
Element Size	3, mm
Sizing	
Use Adaptive Sizi...	Yes
Resolution	7
Mesh Defeaturing	Yes
Defeature Size	Default
Transition	Slow
Span Angle Center	Fine
Initial Size Seed	Assembly
Bounding Box Di...	297,41 mm
Average Surface ...	646,38 mm²
Minimum Edge L...	0,2 mm
Quality	
Inflation	
Advanced	
Statistics	
Nodes	203688
Elements	44640

Figure 4.12: General Mesh Settings

Finally, the mesh used in the analyses can be seen in Figures 4.13 and 4.14.

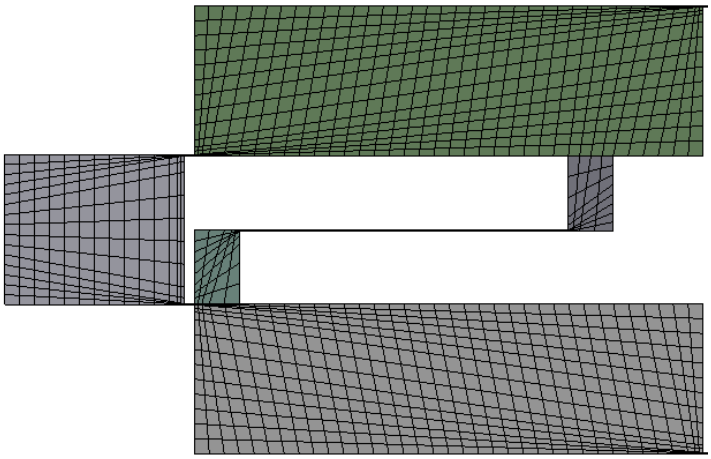

Figure 4.13: General Mesh View 1

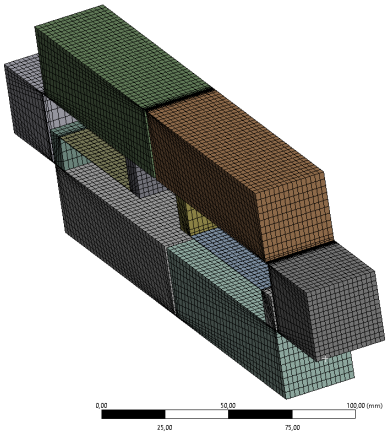

Figure 4.14: General Mesh View 2

4.2.2 Analysis and Results

To start the analysis, firstly, the configuration in [3] was reconstructed and the band gap was verified in ANSYS. The point masses that were present in [3] were not accounted for in this project, therefore the natural frequencies in Figure 2.6 differ from those in our configuration. The mode shapes and the first two natural frequencies in our system can be seen in Figure 4.15.

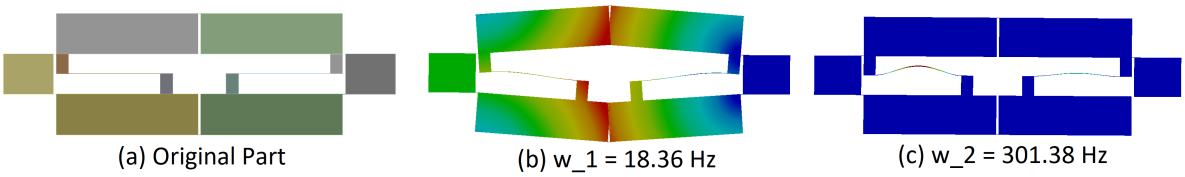

Figure 4.15: Natural frequencies and mode shapes

The weight compensation problem can be quantified with finite element analysis.

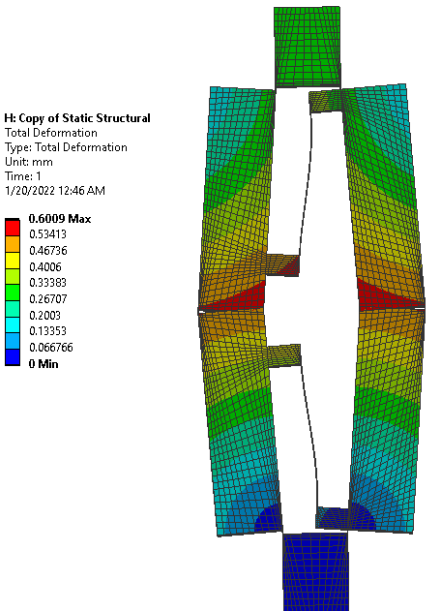

Figure 4.16: Compression under its own weight

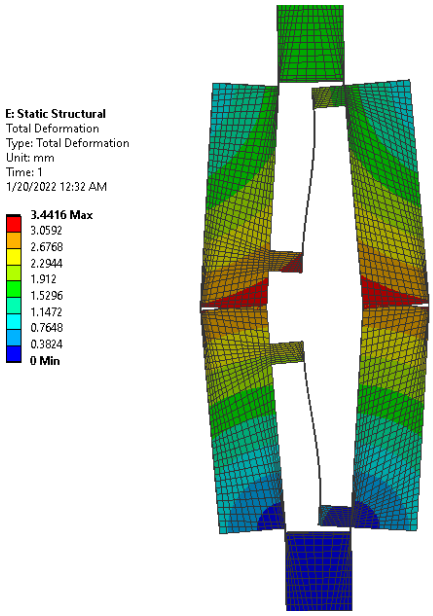

Figure 4.17: 10N External Force added

Figure 4.16 shows the compression of the system under its own weight. This corresponds to Figure 2.7 where the aluminum sigma profiles come into contact in the region with the largest deformation in Figure 4.16. Figure 4.17 shows the compression of the system under the effect of an external force of $10N$ which is the target external force to be compensated in this project. As discussed before, the main compensation mechanism is to use already bent beams (their relaxed shape is permanently deformed) and bring them back to a straight shape and fix them to the supports. This introduces internal forces and moments, which in turn is applied to the whole structure. These resultant forces and moments are the main sources of the weight compensation mechanism. The forces and moments induced by bringing the bent beam to a straight shape are taken to be the same as the forces and moments that would be needed to bend a straight beam. The errors introduced by this assumption were calculated to be small, and since a fine tuning mechanism will be used in the end, it can be justified.

The forces and moments were calculated by fixing one end of the long flexures while giving displacements to the other. First, the reaction forces and moments were checked. Then, the forces and moments (in the opposite direction) were applied to the whole structure with a straight flexure since bringing the flexure to its straight shape would apply forces and moments to the structure. This method of applying forces and moments is illustrated in Figure 4.18.

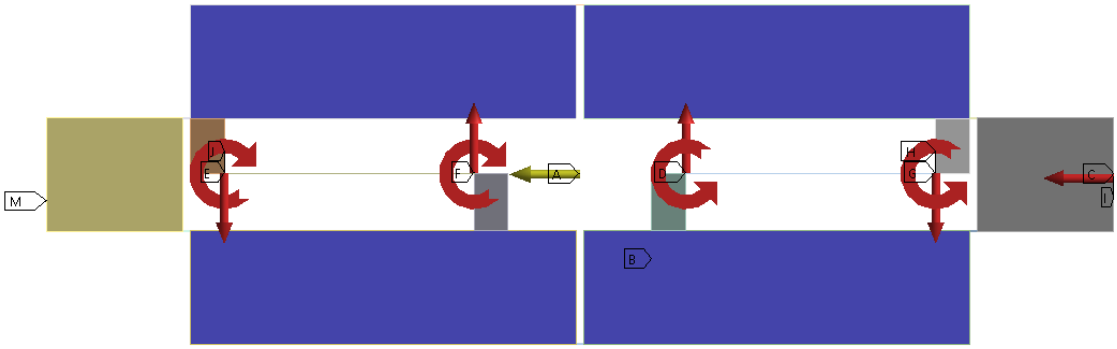

Figure 4.18: The forces and moments applied by the flexure

In Figure 4.18, A (the yellow force) represents the weight, C (the rightmost force) is the externally applied vertical force. All of the other forces (which are applied by the flexures) have the same magnitude, however the moments have different magnitudes. The initial deflection needed in the flexure, the resultant forces and the external force that can be balanced by this deflection are tabulated in Table 2. The moments are omitted in the table but they are included in the calculations.

Table 2: Required horizontal reaction force for negligible deformation

External Force to be balanced	**Required displacement**	**Internal Force**
0	5.9 mm	0.94 N
5 N	12.5 mm	2.99 N
10 N	18.2 mm	4.82 N

The calculation of these required displacements was done in an iterative manner. Firstly, an initial displacement was given to just a flexure, which can be seen in Figure 4.19. Figure 4.19 is the flexure that can balance $10N$ of external load, which is the aim of this project. Then, the resulting reaction forces are applied to the whole system and by examining total deformation at the critical points (which make contact under load), we checked whether the weight compensation is successful or not, as in Figure 4.20. By small increments this process is continued until the deformation is negligible. The effect of the added forces and moments (shown in Figure 4.18) on modal and harmonic response analysis was verified to be negligibly small.

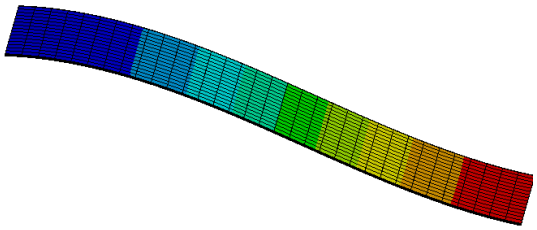

Figure 4.19: 18.2mm deflected beam

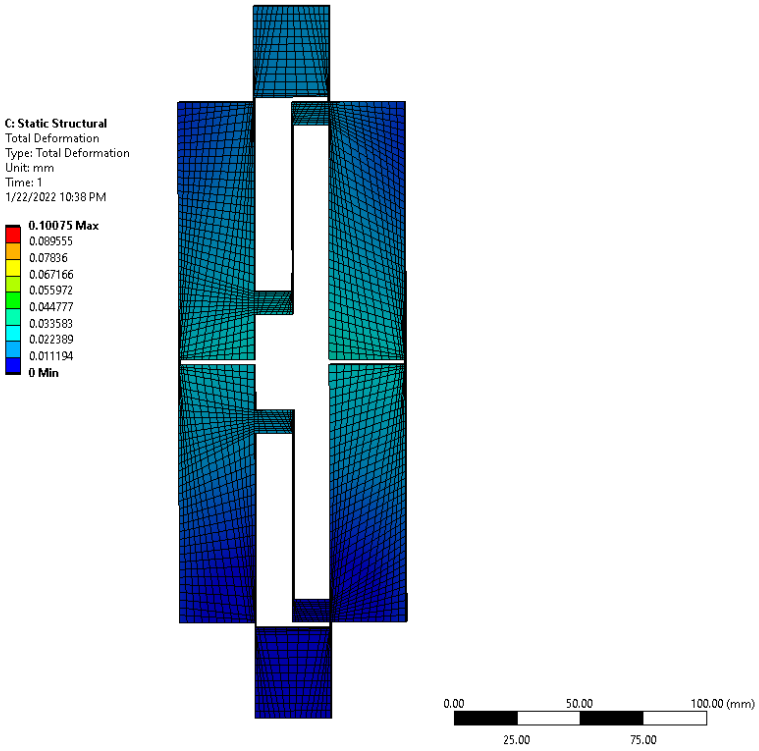

Figure 4.20: Successful weight compensation

The next step is to calculate the effects of a rotation of one end of the flexure on modal and harmonic response analysis, since that will be used for fine tuning. The effect of rotation on weight compensation is to induce forces and moments which enable the structure to carry even more load which will be given in the subsequent sections. However, giving too much rotation comes at the expense of band gap. Therefore, it is going to be used only for fine tuning. To validate that the bang gap is still acceptable after rotating one end of the flexure, modal analyses are conducted for those mechanisms with appropriate support types. In Figures 4.21-4.22 and 4.23, it can be seen that compared to Figure 4.15 wide band gap is mostly preserved up to 17 degrees of rotation.

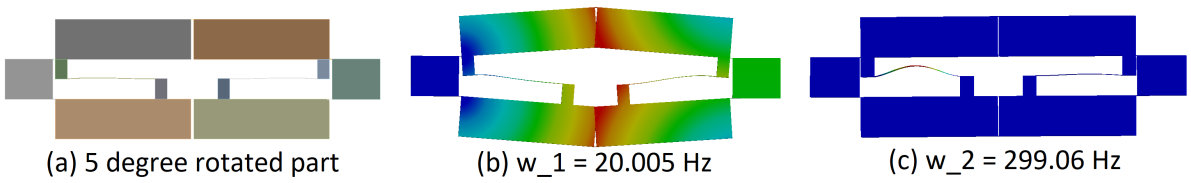

Figure 4.21: Natural frequencies and mode shapes for 5 degrees of rotation

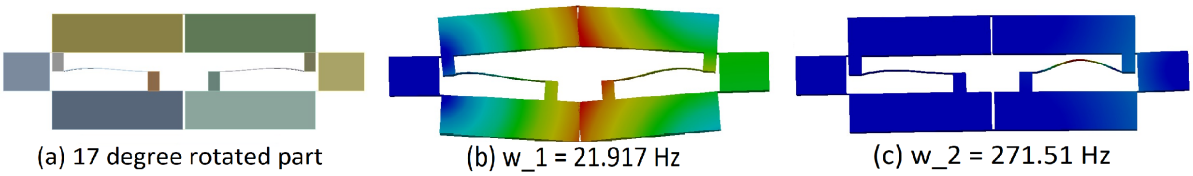

Figure 4.22: Natural frequencies and mode shapes for 17 degrees of rotation

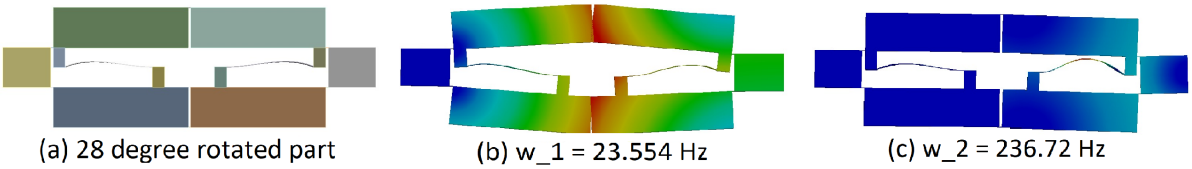

Figure 4.23: Natural frequencies and mode shapes for 28 degrees of rotation

The same behavior can be observed by the harmonic analyses and frequency response plots given in Figures 4.25 through 4.27. 1mm displacement is given from one end of the structure and the resultant displacement at the other end is measured at each frequency. Notice that except for the positions of the peaks at natural frequencies, these plots give values less than 1.

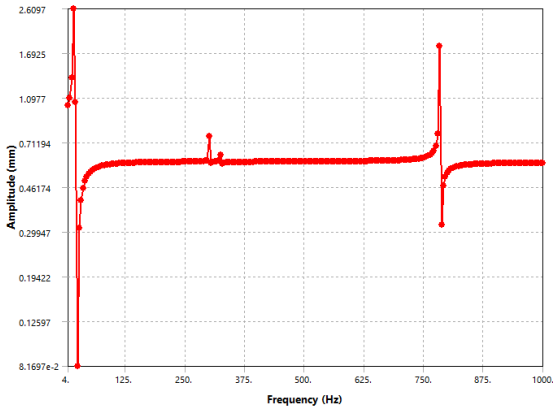

Figure 4.24: Original FRF

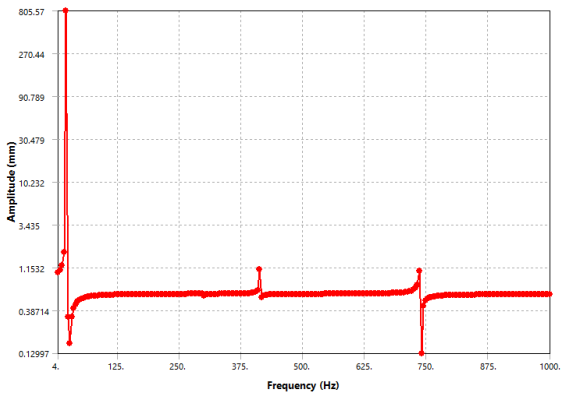

Figure 4.25: 5 degree FRF

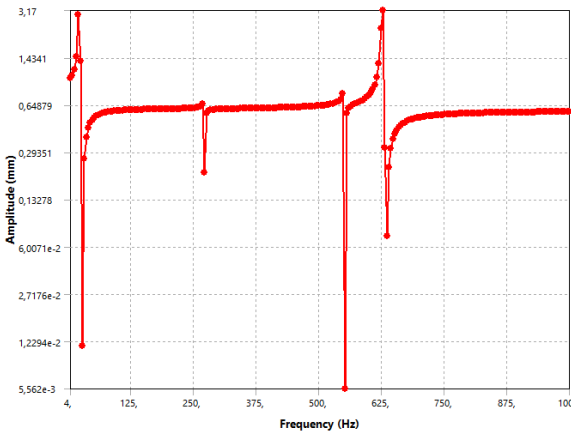

Figure 4.26: 17 degree FRF

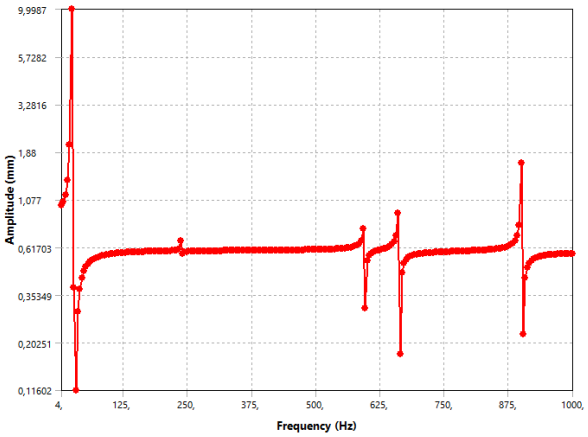

Figure 4.27: 28 degree FRF

4.3 Analytical Formulation

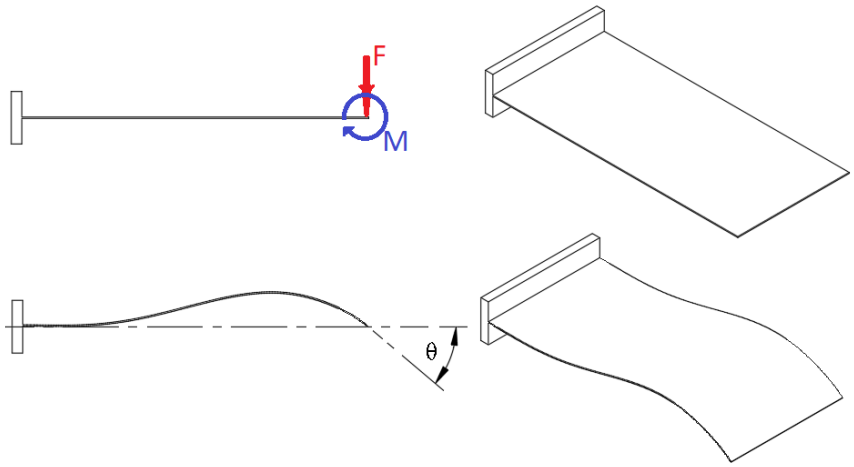

Figure 4.28: Free-Body of deflection of the long flexure

The angle adjustment mechanism which has been discussed in the previous chapters can also be formulated analytically. The system can be uniquely defined by 4 boundary conditions,

$$\delta_a = 0$$

$$\theta_a = 0$$

$$\delta_b = 0$$

$$\theta_b = \theta_0$$

where the subscripts a and b denote the left and right ends of the beam, respectively. In the actual system, one end is fixed completely while the other end is free to rotate. By rotating one end, moments and forces are induced. These can be shown as in Figure 4.28. By using the results of deflection tables from mechanics of materials [6] with one end fixed, the first two boundary conditions above are already satisfied. Using the third and fourth boundary conditions with deflection formulas, one can obtain

$$\delta_b = \frac{FL^3}{3EI} + \frac{ML^2}{2EI} = 0 \tag{1}$$

$$\theta_b = \frac{FL^2}{2EI} + \frac{ML}{EI} = \theta_0 \tag{2}$$

From 1, we have,

$$M = -\frac{2FL}{3} \tag{3}$$

Finally, substitute 3 in 2 to get,

$$F = \frac{6EI}{L^2}\theta_0 \tag{4}$$

$$M = -\frac{4EI}{L}\theta_0 \tag{5}$$

For different θ_0 values, comparison of analytical and finite element methods can be seen in Table 3. For the long flexure used in the system, Young's Modulus, E, is 210 GPa, L is 0.066 m and inertia I is $(30mm \times 0.25^3 mm^3)/12 = 2 \times 10^{-14} m^4$.

Table 3: Comparison of reaction forces for analytical and finite element methods

θ_0 **(Degrees)**	**Analytical Force**	**Finite Element Method Force**
5	0.99 N	0.96 N
17	3.35 N	3.28 N
28	5.52 N	5.4 N

An analytical model for the initially deflected flexure does not give reliable results since the exerted displacement is beyond the applicable range of the deflection formulas. The known deflection formulas were used to be compared to the values in Table 2, however, the analytical results were not even remotely close to those obtained from finite element analysis. A detailed analysis is required but it is beyond the scope of this project.

4.4 Maximum Allowable External Load

The calculations and analyses were made assuming that the externally applied force is 10N, therefore it is optimized to that value. Figure 4.20 shows the structure after the deflected flexure has been installed and fixed. The angle adjusting mechanism which was discussed in the previous chapters is meant to be used for fine tuning. However, the effect of angle adjustment on initial stresses is also significant if the angle is sufficiently high. Some additional loads can be compensated by adjusting the angle of the flexure. From the results of Section 4.2.2, it can be said that 17 degrees of rotation is fairly conservative in terms of preserving the band gap. Therefore, a maximum allowable external load calculation was done assuming that a maximum angle of 17 degrees will be used if needed. A load of 20N in addition to the weight of the structure can be supported if a flexure with 18.2mm displacement is straightened and combined with an angle of 17 degrees.

4.5 Cost Analysis

The weight compensation mechanism is a supplement to the inertial amplification system and it only includes shoulder bolts, nuts and connection parts for shoulder bolts. Expense items for the rest of the system will not be considered in this report. The shoulder bolt needs to be machined with a milling cutter to open the slit at the middle so that the long flexure can be fixed to the axis of the bolt. This application can be conducted at the Vibrations Laboratory at Bogazici University KB222. The connection part for the shoulder bolt can also be machined with Lab resources. So, the only relevant cost is the shoulder bolt for 5-10$ which is not that relevant.

5 Conclusion

In conclusion, the aim of this project was to compensate for the weight of the structure which causes it to malfunction when used in the vertical direction. The structure is expected to take an additional load of 10 N so the weight compensation mechanism must also account for that. Two mechanisms are proposed and proven to be suitable for this problem which requires conservation of the wide band gap. The first mechanism is to use an already bent beam (which is plastically deformed) and bring it back to a straight shape. Straightening the beam and fixing it to the mechanism provides restoring forces and moments that are made use of in weight compensation. This is chosen as the main mechanism simply because its effect on the band gap is negligible. However, the bent flexure mechanism makes use of plastic deformations which require large deflections and it is difficult to obtain such a flexure precisely. This is the main reason for the existence of the second mechanism which serves the purpose of fine tuning. The second mechanism is to give some angular displacement to one end of the fixed flexure to introduce additional internal forces and moments. This mechanism has an adverse effect on the band gap and is only planned to be used for small adjustments in this project. However, this effect is not so significant until about ~ 17 degrees therefore it may also be used to compensate for some additional weight if needed without having substantial drawbacks.

6 References

[1] https://upload.wikimedia.org/wikipedia/commons/thumb/c/c3/Artist%27s_rendition_of_the_new_light-bending_metamaterial.jpg/800px-Artist%27s_rendition_of_the_new_light-bending_metamaterial.jpg

[2] https://upload.wikimedia.org/wikipedia/commons/a/a8/Auxetic_structure.gif

[3] Taniker, S., Yilmaz, C., 2017. Generating ultra wide vibration stop bands by a novel inertial amplification mechanism topology with flexure hinges. International Journal of Solids and Structures 106, 129–138.

[4] Yilmaz, C., Hulbert, G.M., Kikuchi, N., 2007. Phononic band gaps induced by inertial amplification in periodic media. Phys. Rev. B 76 (5), 054309.

[5] Cui P., Li B., Tang J., Gong X., Ma M. (2019) An Improved Tri-linear Interpolation Method for Hybrid Overset Grids and Its Application. In: Zhang X. (eds) The Proceedings of the 2018 Asia-Pacific International Symposium on Aerospace Technology (APISAT 2018). APISAT 2018. Lecture Notes in Electrical Engineering, vol 459. Springer, Singapore. https://doi.org/10.1007/978-981-13-3305-7_49

[6] J. M. Gere, Mechanics of Materials, CENGAGE Learning, 2013, p. 760.

In this project ANSYS Academic is used.

A Technical Drawings

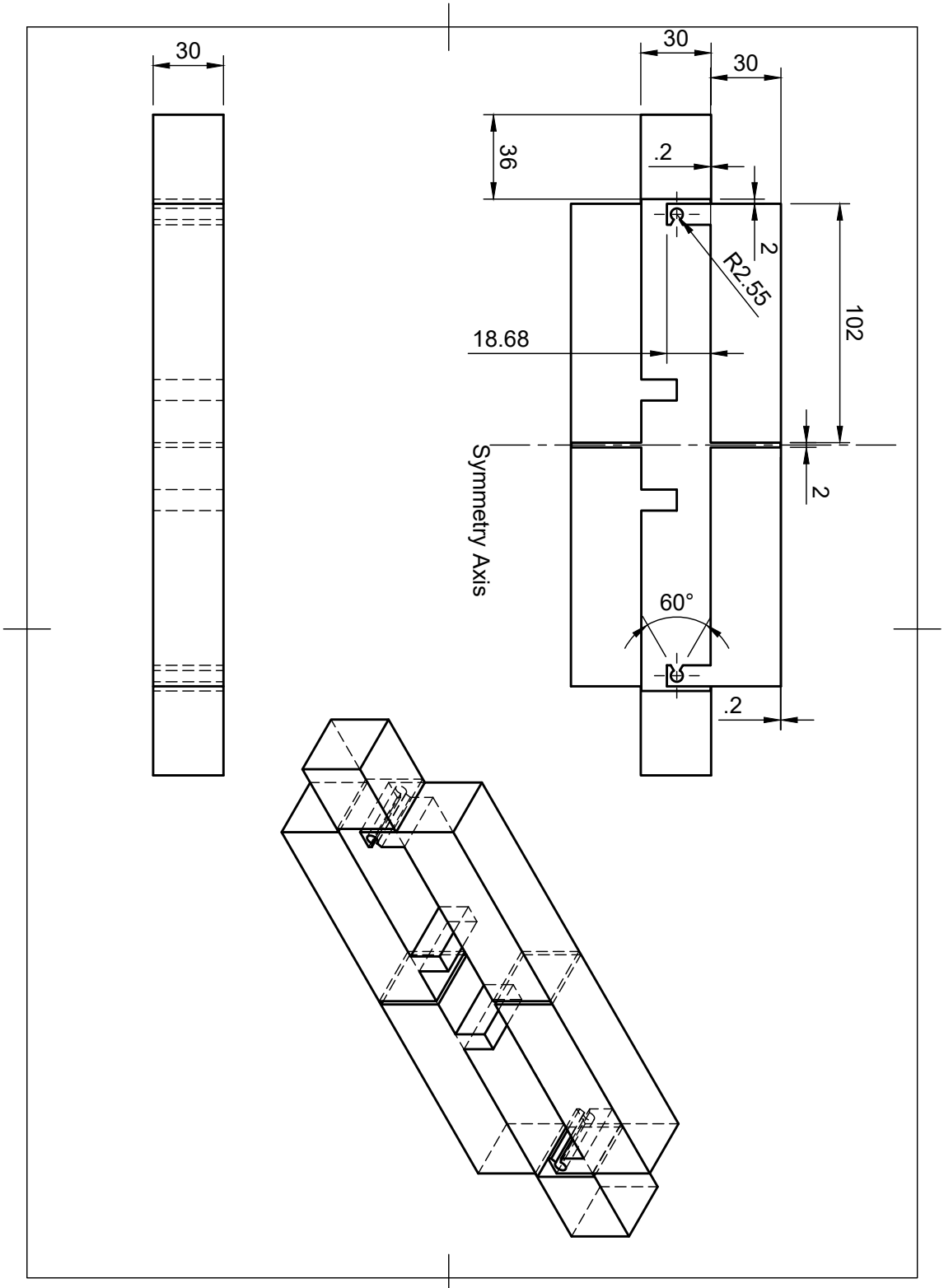

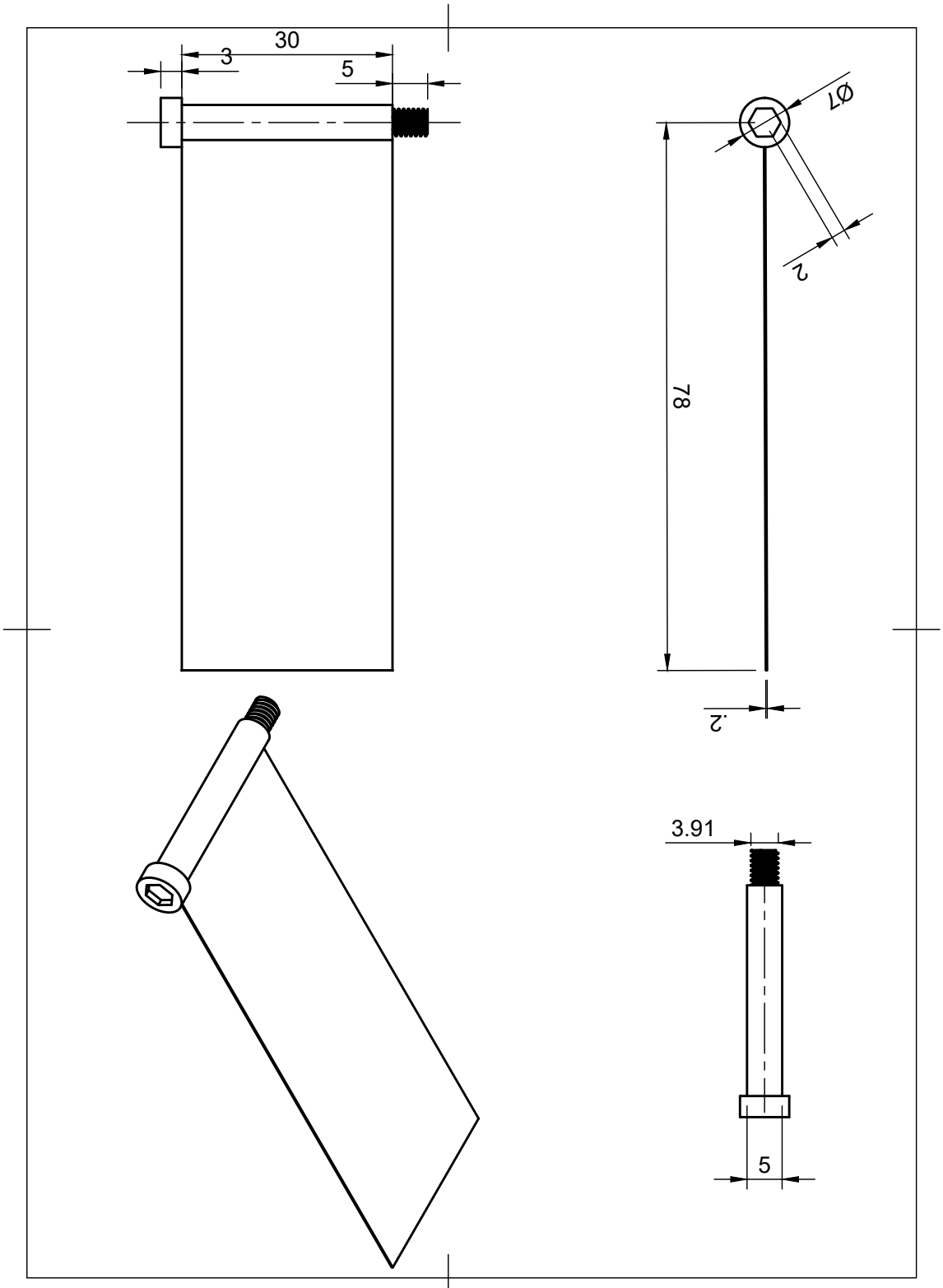
30
3
5
Ø7
2
78
.2
3.91
5